Global change in action due to trapping: How to derive it whatever the rate of variation of the dynamics

Didier Bénisti[*] and Laurent Gremillet

CEA, DAM, DIF F-91297 Arpajon, France

In this paper, we investigate the motion of a set of charged particles acted upon by a growing electrostatic wave in the limit when the initial wave amplitude is vanishingly small and when all the particles have the same initial action, I_0. We show, both theoretically and numerically, that when all the particles have been trapped in the wave potential, the distribution in action exhibits a very sharp peak about the smallest action. Moreover, as the wave keeps growing, the most probable action tends toward a constant, I_f, which we estimate theoretically. In particular, we show that I_f may be calculated very accurately when the particles' motion before trapping is far from adiabatic by making use of a perturbation analysis in the wave amplitude. This fills a gap regarding the computation of the action change, which, in the past, has only been addressed for slowly varying dynamics. Moreover, when the variations of the dynamics are fast enough, we show that the Fourier components of the particles' distribution function can be calculated by connecting estimates from our perturbation analysis with those obtained by assuming that all the particles have the same constant action, $I = I_f$. This result is used to compute theoretically the imaginary part of the electron susceptibility of an electrostatic wave in a plasma. Moreover, using our formula for the electron susceptibility, we can extend the range in ϵ_a (the parameter that quantifies the slowness of the dynamics) for our perturbative estimate of $I_f - I_0$. This range can actually be pushed down to values of ϵ_a allowing the use of neoadiabatic techniques to compute the jump in action. Hence, this paper shows that the action change due to trapping can be calculated theoretically, regardless of the rate of variation of the dynamics, by connecting perturbative results with neoadiabatic ones.

I. INTRODUCTION

As is well known [1], for the nearly periodic and slowly varying dynamics of a Hamiltonian, $H(x,v,\varepsilon t)$, the action I defined as the area enclosed by a frozen orbit [i.e., an orbit of the Hamiltonian $H(x,v,\varepsilon t_0)$, where t_0 is a constant] is an adiabatic invariant. Nevertheless, it is also well known [2,3] that the crossing of a separatrix (i.e., a frozen orbit that contains an unstable fixed point) breaks the adiabatic invariance, and the change in action, which quantifies the accuracy of the adiabatic approximation, has been studied extensively due to its relevance to many fields of physics. To cite a few examples, action-variation calculations, and the adiabatic approximation itself, have been used in transport theory (see Refs. [4,5] and references therein), celestial mechanics (see, for example, Ref. [6]), accelerator physics [7], Bose-Einstein condensates (see Ref. [8] and references therein), and the nonlinear propagation of an electrostatic wave in a plasma (see, for example, Refs. [9–15]) with an application to stimulated Raman scattering [16,17]. With regard to the latter application, which motivated the present work, separatrix crossing occurs due to the trapping of electrons in the potential of an essentially growing electrostatic wave. This led us to focus, in this paper, on the motion of particles in an exponentially increasing potential, and, for this important physics situation, we completely revisit the change in action, ΔI, due to trapping. Indeed, we believe that the analysis we are presenting here significantly differs from the previous numerous publications on the subject in several respects.

First, we provide a theoretical estimate of ΔI for a non-slowly-varying dynamics, i.e., when the particles' motion

before trapping is far from adiabatic. This fills a gap regarding the computation of the action change, which, as far as we know, has always been performed within the framework of the neoadiabatic theory [1–3], which is only useful for slowly varying dynamics. Consequently, as shown in Fig. 6, we are able to estimate ΔI when it is *not* small compared to the initial action. At this point, one may wonder about the relevance of the action, I, for a non-slowly-varying Hamiltonian dynamics, when the very notion of adiabatic invariance seems meaningless. Actually, for the adiabatic approximation to be valid, the period of a frozen orbit must be small compared to the typical time of variation of the Hamiltonian. Now, the period of a trapped orbit typically decreases as the square root of the potential amplitude so that, if this amplitude keeps growing, eventually the variations in the action will become very small. Moreover, as we will show in this paper, and as illustrated in Fig. 2, if the growth rate is large enough, then, by making use of a perturbation analysis in the potential amplitude, we are able to solve the equations of motion up to a time, t_1, when the amplitude is large enough for the action to remain nearly constant when $t > t_1$. Therefore, for large enough growth rates, perturbative results may be connected with adiabatic ones to provide an accurate solution of the equations of motion. In particular, as explained in Ref. [18], this procedure yields the particles' distribution function at any time, for a nonintegrable dynamics when the classical methods of the neoadiabatic theory do not apply. This shows the importance of computing the jump in action, ΔI.

Second, we do not focus here on the microscopic description of the change in action for each particle; instead, we want to show how ΔI may be used to compute macroscopic, or averaged, quantities. To do so, we address the relevance of defining, at any time, one single action, $I^*(I_0)$, for a *set*

─────────
*didier.benisti@cea.fr

of particles having all the same initial action, I_0. Hence, by "global change in action" we mean here the change in $I^*(I_0)$, provided that this quantity is meaningful. Clearly, the concept of a "global action" for a set a particles, which we want to introduce here, would be exact if the distribution in action, $f(I,t)$, remained a Dirac distribution at any time, i.e., $f(I,t) = \delta(I - I^*)$. Therefore, we start by investigating if, and when, $f(I,t)$ has just one very sharp peak about a given action, I^*. Then, we study the convergence of I^* toward an asymptotic value, I_f, as the wave amplitude keeps growing, and we define the global change in action as $\Delta I \equiv I_f - I_0$.

Third, we test the usefulness of the concept of global action to compute one particular macroscopic quantity, χ_i, which is the imaginary part of what may be viewed as a generalized electron susceptibility for a plasma wave. Our definition for the generalized susceptibility, χ, is given by Eq. (11) of Sec. III, showing that χ is proportional to the ratio between the amplitude of the charge density and that of the wave. Then, Gauss law just translates into $1 + \chi = 0$, so that, necessarily, $\chi_i = 0$. As discussed in several papers (e.g., Refs. [10–13,15–17]), the latter equation may be used to derive such basic and important quantities as the nonlinear Landau damping rate of a plasma wave, and, more generally, to describe very accurately the nonlinear propagation of such a wave. This is also true when the wave is laser-driven, so that, once the nonlinear variations of χ_i are known, one may address the nonlinear stage of stimulated Raman scattering, which has proven to be an issue for inertial confinement fusion [19]. We will not discuss here any of these points, which are beyond the scope of this paper, and which will be the subject of a forthcoming article. Nevertheless, as an application of our results, we will show how to compute χ_i for an exponentially growing wave. This will actually let us estimate ΔI for a larger range in ε_a, the parameter that quantifies the slowness of the dynamics, than by directly resorting to the distribution function, and, actually, down to values of ε_a within the range of validity of the neoadiabatic theory. Hence, one important result of this paper is to show that the change in action due to trapping may be accurately estimated, regardless of the rate of variation of the dynamics, by connecting results from a perturbation analysis in the wave amplitude with those from the neoadiabatic theory.

Note that, in this paper, we focus on the asymptotic variation in action, $\Delta I \equiv I_f - I_0$, due to trapping so that, by "global change in action" we also mean the "total action variation" due to trapping. However, we also investigate the shift in action, δI_S, experienced by the particles once they have come close to the frozen separatrix. In particular, we investigate how δI_S scales with ε_a, and we compare this scaling with that of ΔI.

The previous points, which are the main results of our paper, are presented the following way. In Sec. II, we introduce the Hamiltonian dynamics that will be studied throughout the paper, and we define what we will consider as the parameter, ε_a, that quantifies the slowness of the dynamics, and that usually is the small parameter of the neoadiabatic theory (but which is not necessarily small here). When ε_a is larger than unity, we show that a perturbation analysis in the wave amplitude may accurately describe the orbits in phase space up to the point when the amplitude is so large that the wave has trapped almost all the particles in its potential. Using this result, we can very easily predict the main features of the distribution in

action, $f(I,t)$, when $f(I,t = 0) = \delta(I - I_0)$. In particular, we can discuss when, and why, $f(I,t)$ should exhibit one single peak, about a given value I^*, which happens to be the smallest action. Moreover, the main results obtained theoretically for $f(I,t)$ when $\varepsilon_a \gtrsim 1$ are numerically shown to remain valid when $\varepsilon_a < 1$, particularly with regard to the fact that $f(I,t)$ eventually exhibits one single peak about I^*. The latter point is actually expected since, as we will show in Sec. II, it agrees with the predictions of the neoadiabatic theory. The values of I^* derived by making use of a perturbation analysis are compared to those calculated numerically, with an emphasis on the ability to correctly estimate the asymptotic value, I_f, reached by I^* as the wave keeps growing. The comparison between the numerical and theoretical values of I_f actually sets the limit, in ε_a, for the direct use of a perturbation analysis. The scaling of $\Delta I \equiv I_f - I_0$ with ε_a, in the limit $\varepsilon_a \to 0$, is also investigated numerically and compared to that obtained by making use of the neoadiabatic theory. Numerically, we also investigate the change in action, $\delta I_S \equiv I^* - I_0$, when the particles are very close to the frozen separatrix, and the scaling of δI_S with ε_a is compared with that of ΔI. In Sec. III, we show that when ε_a is large enough, the imaginary part, χ_i, of the electron susceptibility of an electrostatic wave in a plasma may be accurately estimated by connecting perturbative results with those obtained by assuming that all the particles have the same constant action, $I = I_f$. Comparisons between the numerical and theoretical values of χ_i actually provide another diagnostic with regard to the accuracy of our prediction for I_f. Moreover, since χ_i is more easily and more accurately computed than the distribution in action, it can be used to yield precise estimates of I_f for a larger range in ϵ_a than in Sec. II. In particular, we show that these perturbative estimates remain accurate down to values of ε_a within the range of validity of the neoadiabatic theory. Finally, Sec. IV summarizes and concludes this work.

II. THE GLOBAL CHANGE IN ACTION

A. The considered dynamics

In the remainder of this paper, we will study the motion of particles in an exponentially growing sinusoidal potential, as given by the Hamiltonian

$$H_1 = \frac{p^2}{2} - A_0 e^{\varepsilon \tau} \cos(x). \tag{1}$$

This choice was mainly motivated by issues regarding nonlinear wave-particle interactions in plasma physics [20], which will be discussed briefly in Sec. III.

At first glance, it seems natural to use ε, the wave growth rate, in order to quantify the slowness of the dynamics, and to study how the change in action scales with ε, as done, for example, in Ref. [3]. However, it is more accurate to use $\varepsilon_a = \varepsilon/p_0$, where p_0 is the initial value of p, since this represents the ratio between the period of a frozen orbit and the typical time of variation of the dynamics. Indeed, the period of an untrapped orbit, far from the separatrix, scales as $1/p_0$, while for a nearly adiabatic motion, an orbit is trapped when $\sqrt{A} \gtrsim \pi p_0/4$ [10] (where $A \equiv A_0 e^{\varepsilon \tau}$), and the period of this orbit then scales as $1/\sqrt{A}$. With this in mind, we now make the change of variables $t = \varepsilon \tau$, $v = p/\varepsilon$, and, in these new variables, the dynamics of

H_1 is given by

$$H = \frac{v^2}{2} - \Phi_0 e^t \cos(x), \qquad (2)$$

where $\Phi_0 = A_0/\varepsilon^2$ [21]. The slowness of the dynamics defined by H is quantified by $\varepsilon_a = 1/v_0$, where v_0 is the initial value of v. Moreover, in the limit when $\Phi_0 \to 0$, which we will consider here, the initial action, I_0, is just $I_0 = v_0$, since

$$I = \frac{1}{2\pi} \oint v \, dx, \qquad (3)$$

where the integral is over a frozen orbit, provided that this orbit is untrapped [for a trapped orbit, I is defined as one-half of the value given by Eq. (3) in order to avoid a jump in action only due to geometrical effects]. We therefore conclude that $\varepsilon_a = 1/I_0$.

Note that if, for the dynamics of H_1, the change in action scales as ε, then the change in action for the dynamics defined by H is just a constant, independent of ε_a. Moreover, a change in action proportional to $\varepsilon \ln(\varepsilon)$ for the dynamics of H_1 would translate into an action change proportional to $\ln(\varepsilon_a) = -\ln(I_0)$ for the dynamics of H.

In the remainder of this paper, we will focus on the dynamics of H in the limit $\Phi_0 \to 0$, and we will simply study the change in action as a function of I_0.

B. The distribution in action

Let us now investigate the distribution in action, $f(I)$, for a set of particles with the same initial action, I_0 (i.e., the same initial velocity), and whose positions are uniformly distributed between 0 and 2π. Since we consider the limit $\Phi_0 \to 0$, it is possible to describe the particles' motion, up to a certain time, by making use of a perturbation analysis in the amplitude of the potential, $\Phi \equiv \Phi_0 e^t$. This has actually been done in Ref. [10], where it has been shown that $\varepsilon_p = \Phi/(1 + I_0^2)$ may be chosen as the small parameter of the perturbative expansion, which should therefore provide accurate results when $\Phi \ll (1 + I_0^2)$. Now, as regards the change in action, it mainly occurs when the orbit is close to the frozen separatrix, i.e., when $\Phi \sim I_0^2$, so that I should remain nearly constant once $\Phi \gg I_0^2$. Hence, when I_0 is sufficiently small compared to unity, is should be possible to use a perturbation analysis to derive the distribution in action up to the point when this distribution remains nearly stationary. Therefore, as explained in Ref. [20], by connecting perturbative results with adiabatic ones, it is possible to derive the particles' distribution function at any time. However, in this paper, we shall pursue another goal, which is the derivation of macroscopic quantities, such as moments or Fourier components of the distribution function, that are usually enough to address self-consistent physics problems, such as the nonlinear propagation of waves in a plasma. Now, it is not necessary to go through the precise microscopic description of the distribution function to derive macroscopic quantities, and this would actually be very ineffective. To make this point more transparent, we start by investigating the main properties of the action distribution function, $f(I)$.

When the amplitude, $\Phi \equiv \Phi_0 e^t$, is so small that no particle is trapped in the potential, i.e., when

$$m \equiv \frac{H + \Phi}{2\Phi} \qquad (4)$$

is larger than unity for all particles, $f(I)$ exhibits two sharp peaks located at the minimum and maximum action. This may be seen in Fig. 1(a) comparing the perturbative results with those obtained numerically by directly solving the equations of motion with a symplectic leapfrog integrator [22]. Numerically, we choose $\Phi_0 = 10^{-8}$, we consider 1000 particles, and we initialize them with the hypothesis that, when $\Phi_0 \to 0$, all the particles have the same velocity (or, equivalently, the same action, I_0) and that their positions, x_0, are uniformly distributed between 0 and 2π (see Ref. [10] for details). As may be seen in Fig. 1, when no particle is trapped, the perturbative analysis (led, here, up to order 12 [23]) is very accurate, and lets us understand very easily why the distribution in action has two sharp peaks. Indeed, from a perturbative expansion, and for each amplitude, Φ, one can express the action of any particle as a function of its initial position, x_0, and of its initial velocity. Since we consider here the situation when all the particles have the same initial velocity and when x_0 is uniformly distributed between 0 and 2π, we conclude that the distribution function in action, $f(I)$, should just be proportional to $(\partial I/\partial x_0)^{-1}$. Therefore, if the function $I(x_0)$ has some extrema, $f(I)$ should be very peaked about each of these extrema. Now, we find that the function $I(x_0)$ calculated perturbatively has just one maximum and one minimum, which explains why $f(I)$ has exactly two peaks about the minimum and maximum action. These two peaks have nearly the same amplitude, although the one located at the maximum action is a bit higher, so that, for the corresponding values of Φ, the most probable action, I^*, is the maximum one.

As the amplitude, Φ, keeps on increasing, more and more particles are trapped in the potential, i.e., they are such that m, as defined by Eq. (4), is less that unity. Even in the situation when a large fraction of particles are trapped, the perturbative analysis describes very accurately the distribution in action, as may be seen in Fig. 1(c), and it gives a very good approximation of the orbit in phase space, as shown in Fig. 2. Hence, even when a large amount of particles are trapped, by using the same argument as before, we conclude that $f(I)$ should have two sharp peaks about the minimum and maximum actions, which is indeed the case as illustrated in Fig. 1(b). However, these two peaks do not have the same height because, now, the minimum action is for the trapped particles while the maximum action is for the untrapped ones, so that the relative amplitude of the two peaks is just proportional to the relative abundance of these two distinct types of particles. Hence, perturbative results tell us that, as Φ keeps on increasing and more and more particles are getting trapped, the peak in $f(I)$ located at the minimum action becomes more and more prominent while that located at the maximum action tends to vanish. Now, when $I_0 \lesssim 1$, the perturbative analysis can be led up to the point when nearly all the particles are trapped in the potential so that $f(I)$ exhibits one single peak at the minimum action, $I_{\min}$ [see Fig. 1(c)]. At this point, the particles with $I = I_{\min}$ are deeply trapped, i.e., they are far away from the frozen separatrix, so that, as Φ keeps on increasing, their action does not vary much, and $f(I)$
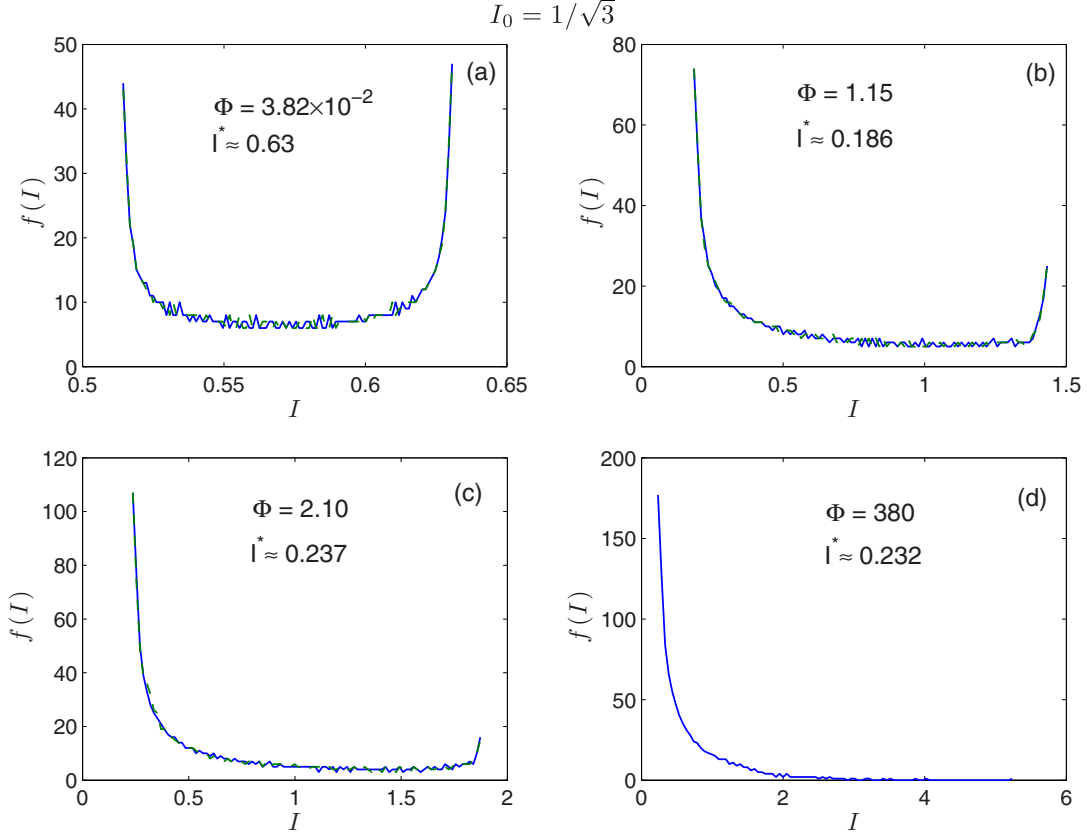
FIG. 1. (Color online) Distribution in action, $f(I)$, when $I_0 = 1/\sqrt{3}$ and for different values of Φ. In panels (a), (b), and (c), the blue solid line represents the distribution obtained numerically, and the green dashed line represents that calculated perturbatively. In panel (d), only the numerical distribution function is plotted since a perturbation analysis is no longer valid for such a large amplitude. In each panel, the value of the most probable action, I^*, is indicated.

keeps one single peak at $I = I_{min}$, as shown in Fig. 1(d). Note that, in Fig. 1(c) for $\Phi = 2.1$, $I_{min} \approx 0.237$, while in Fig. 1(d) for $\Phi = 380$, $I_{min} \approx 0.232$. Therefore, when $I_0 \lesssim 1$, we are able to prove that, eventually, once all the particles have been trapped in the potential, $f(I)$ has one single sharp peak at the value, $I = I_{min}$, that remains nearly constant.
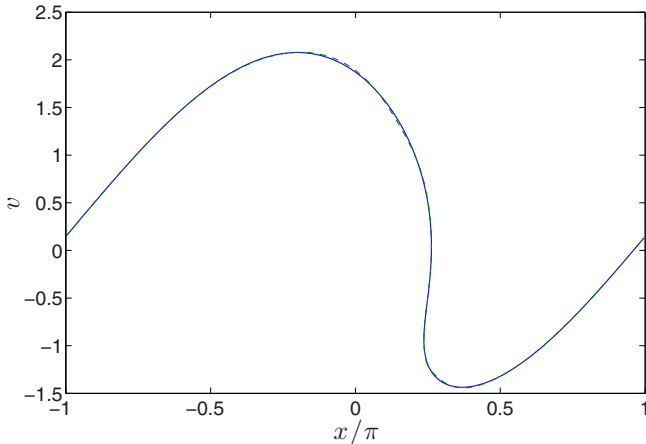

FIG. 2. (Color online) Orbit in phase space calculated numerically (blue solid line) and perturbatively (green dashed line) when $I_0 = 1/\sqrt{3}$ and $\Phi = 2.1$. For these parameters, more than 97% of the particles are trapped in the potential, i.e., they are such that $m < 1$.

For larger values of I_0, we resort to numerical simulations in order to study the variations of $f(I)$, as Φ increases. Figures 3(a)–3(c) show the evolution of $f(I)$ with Φ when $I_0 = 10$. When Φ is so small that most particles are untrapped and perturbative results are accurate, then, for the same reason as before, $f(I)$ has two sharp peaks about the minimum and maximum actions. For intermediate values of Φ, when most particles are trapped and the perturbative expansion is no longer valid, then, as may be seen in Fig. 3(b), a new peak in $f(I)$ may appear for an action slightly larger than the minimum one, a feature that is found numerically and that cannot be explained with the theoretical arguments used when $I_0 \lesssim 1$. Nevertheless, as Φ keeps on increasing, and for all the cases we investigated numerically, we found that, eventually, $f(I)$ exhibited only one sharp peak and that the most probable action, I^*, was also the minimum one.

The latter result is actually expected for large values of I_0 from the neoadiabatic theory. Indeed, from Eq. (83) of Ref. [3], we conclude that, as Φ increases, the action of any particle should converge to the value I_∞ given by

$$I_\infty = I_0 - (2/\pi) \ln |2\pi \sin(h_0/I_0)|, \qquad (5)$$

where h_0 is the value of $(H - \Phi)$ when the particle crosses the line $x = \pi$ (modulo 2π) for the last time before being trapped in the potential. The values of h_0 may be found by using Eqs. (2.12), (2.17), and (2.19) of Ref. [24]. These equations
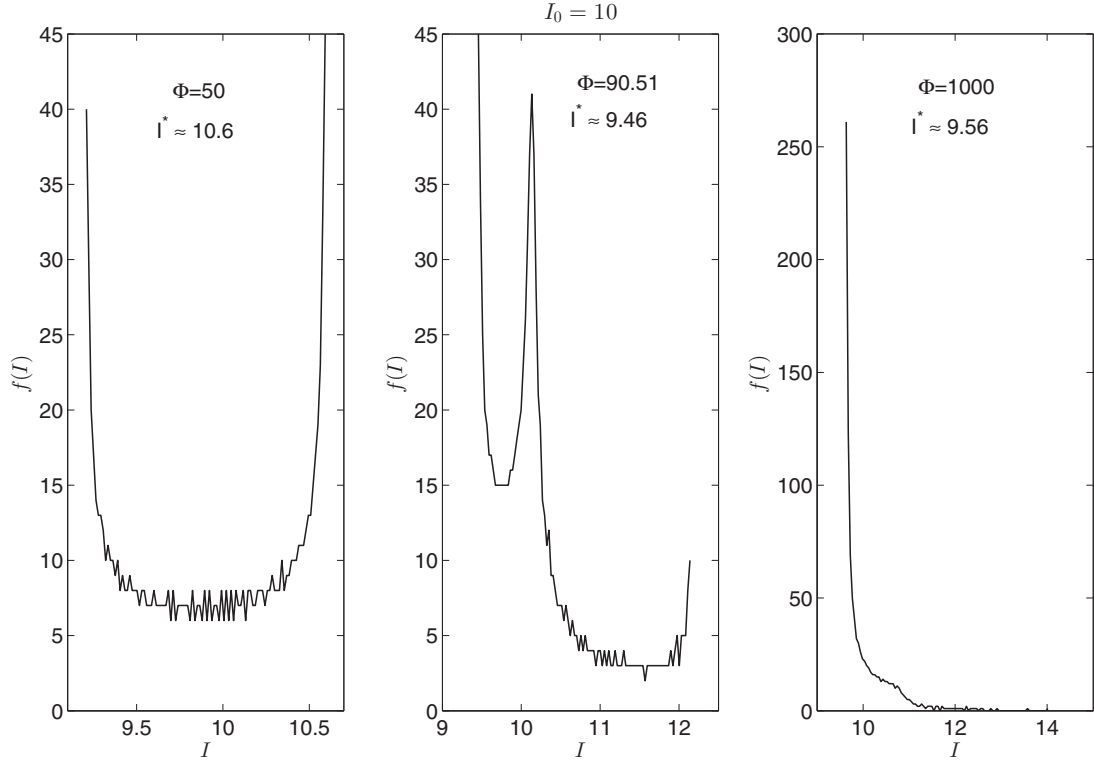
FIG. 3. Distribution in action, $f(I)$, found numerically when $I_0 = 10$ and for various values of Φ.

let us conclude that, for the case considered in this paper, with positions uniformly distributed between 0 and 2π in the limit $\Phi \to 0$, $h_0 = -\pi I_0 u$, where u is uniformly distributed between zero and unity. Plugging this expression for h_0 into Eq. (5), we find

$$I_\infty = I_0 - (2/\pi) \ln |2\pi \sin(\pi u)|, \qquad (6)$$

which clearly shows that I_∞ has only one extremum, which actually is an absolute minimum. Since u is uniformly distributed, we conclude that neoadiabatic theory does predict that $f(I)$ should eventually exhibit only one peak at the minimum action. Moreover, Eq. (6) provides an explicit simple expression for the asymptotic value, I_f, of the most probable action, $I_f = I_0 - (2/\pi) \ln(2)$. We therefore conclude that, for large enough values of I_0, the global change in action, $\Delta I \equiv I_0 - I_f$, as predicted by the neoadiabatic theory, is

$$\Delta I = -(2/\pi) \ln(2) \approx -0.441, \qquad (7)$$

a result we shall now check numerically in Sec. II C. Note that ΔI given by Eq. (7) is independent of I_0, meaning that, if one used Hamiltonian H_1 given by Eq. (1), one would find that the action change would scale as ϵ in the limit $\epsilon \to 0$.

C. Asymptotic value of the most probable action

The typical evolution of the most probable action, I^*, as a function of the wave amplitude, Φ, is plotted in Fig. 4 when $I_0 = 1$. For small values of Φ, $I^* > I_0$, and it slightly increases with Φ because, for such small amplitudes, when most particles are untrapped, then, as explained in Sec. II B, I^* is the maximum action.

A sudden jump, δI, occurs in I^* when most particles are trapped so that I^* no longer is the maximum action but the minimum one. Therefore, δI is the difference between the maximum and minimum action, hence the spread in action, when the particles are close to the frozen separatrix. As shown in Fig. 5, δI scales as $\ln(I_0)$, when $I_0 \gtrsim 10$ [which means that, for the Hamiltonian H_1 given by Eq. (1), the spread in action would scale as $\varepsilon \ln(\varepsilon)$]. Figure 5 shows that the change in action, δI_S, for particles close to the separatrix, either trapped or untrapped, also scales as $\ln(I_0)$. Hence, although studying δI_S in detail is beyond the scope of this paper, it is important to note that the total change in action, ΔI, is not
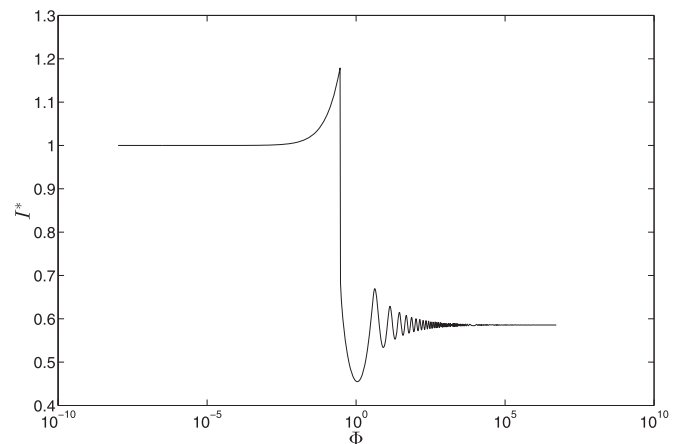
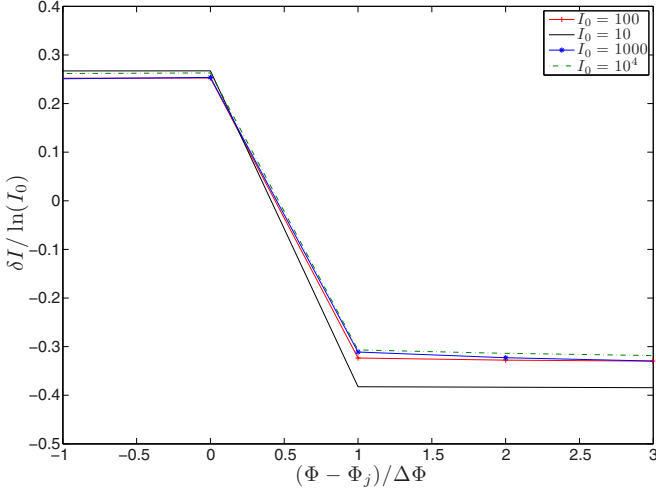FIG. 4. Evolution of the most probable action, I^*, with Φ when $I_0 = 1$.

FIG. 5. (Color online) Jump, δI, in the most probable action divided by $\ln(I_0)$ when $I_0 = 10$ (black solid line), $I_0 = 100$ (red solid line with pluses), $I_0 = 1000$ (starred blue solid line), and $I_0 = 10^4$ (green dashed line). The amplitude, Φ, has been centered about the value, Φ_j, where the jump occurs, and rescaled so that, for our numerical data, we see a jump in I^* when the amplitude changes by one unity.

the maximum action shift experienced by the particles as Φ increases. Actually, ΔI, as predicted by Eq. (7), does not even scale with I_0 as the maximum action shift.

After the jump, I^* exhibits some oscillations of smaller and smaller amplitude and therefore seems to converge toward an asymptotic value, I_f, as the amplitude of the potential keeps on increasing. We now investigate how accurately I_f may be estimated theoretically by making use of a perturbative expansion. When doing so, we cannot take the limit $\Phi \to \infty$, because the perturbative expansion is limited to a finite range of amplitudes. Therefore, we identify I_f with the value of the most probable action, I^*, at a given amplitude, Φ_M, large enough for $I^*(\Phi)$ to remain nearly constant when $\Phi > \Phi_M$, and yet small enough to remain within the range on validity of the perturbative analysis. Since we want to apply our results on the action change to the computation of χ_i, the imaginary part of the electron susceptibility defined by Eq. (11) of Sec. III, we choose Φ_M as the amplitude when χ_i reaches its first maximum. Indeed, as we shall show in Sec. III, after reaching its first maximum, χ_i oscillates with Φ in a very regular fashion, thus reflecting the nearly adiabatic motion of the trapped particles, i.e., the near constancy of their action. As may be seen in Fig. 6, when $I_0 \lesssim 1$, the perturbative value of I^* at the amplitude when χ_i reaches its first maximum is in excellent agreement with the numerical one, and it does indeed provide a very good estimate of I_f, which is only underestimated by about 5%. Hence, as is clearly shown in Fig. 6, we are indeed able to precisely calculate the global change in action due to trapping, $\Delta I \equiv I_f - I_0$, even when this change is of the order of the initial action.

As may be already guessed from Fig. 6(a), and is obvious in Fig. 7, the global change in action, $\Delta I = I_f - I_0$, converges
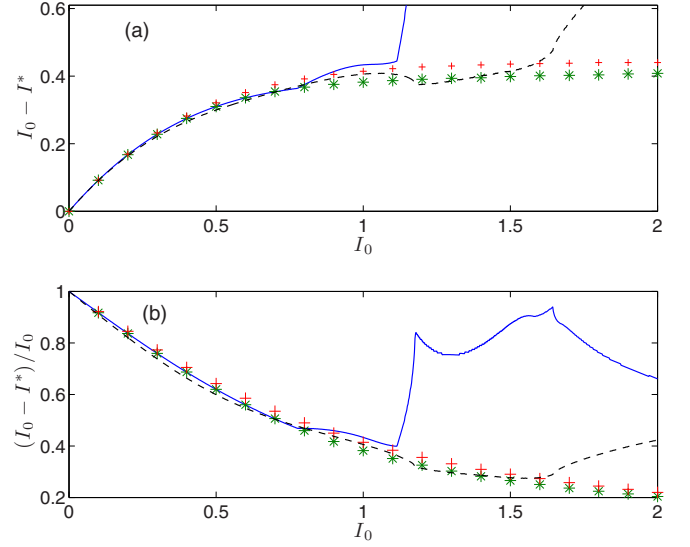

FIG. 6. (Color online) Panel (a), change in action, $I_0 - I^*$, as a function of I_0. The blue solid line plots this change when I^* is derived from the perturbative distribution function calculated when χ_i reaches its first maximum. The green stars also correspond to values of I^* at the first maximum of χ_i, but they are deduced from the distribution function calculated numerically. The black dashed line also refers to I^* at the frst maximum of χ_i, and it is evaluated by making use of Eq. (29) of Sec. III. The red pluses plot $(I_0 - I_f)$ as estimated numerically. In panel (b), the relative change in action, $(I_0 - I^*)/I_0$, is plotted with the same conventions as in panel (a).

toward a constant as $I_0 \to \infty$. Numerically, this constant is found to be very close to -0.44 (see also Figs. 9 and 10), which is in excellent agreement with the prediction of Eq. (7) from neoadiabatic theory. Note also that the convergence of ΔI toward a constant occurs quite rapidly since we numerically estimate that, when $I_0 = 1$, $\Delta I \approx -0.414$ [which departs by less than 10% from the asymptotic value of Eq. (7)], while when $I_0 = 1.6$, $\Delta I \approx -0.437$ [which departs by less than 1% from the asymptotic value of Eq. (7)].
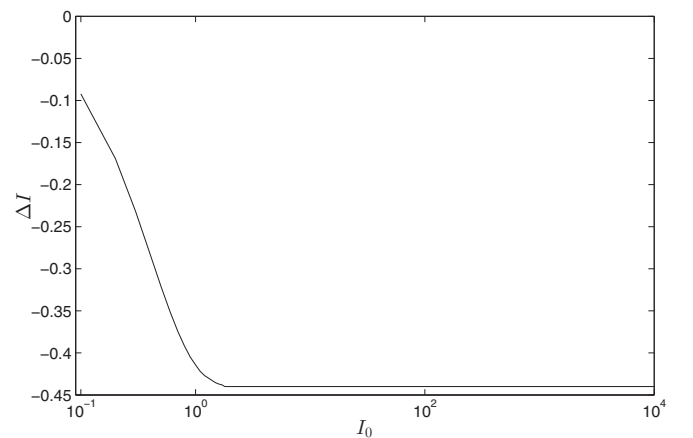

FIG. 7. Global change in action, $\Delta I = I_f - I_0$, as a function of I_0.

III. APPLICATION TO THE DERIVATION OF THE IMAGINARY PART OF THE ELECTRON SUSCEPTIBILITY FOR AN ELECTROSTATIC WAVE IN A PLASMA

In Sec. II, we showed that we could provide a theoretical estimate for the global change in action, ΔI, when it was not small compared to the initial action, i.e., when the classical techniques of the neoadiabatic theory did not apply. However, to do so, we had to use a perturbation analysis up to order 12, and the corresponding formulas are pages long so that, although it is important to provide theoretical results, one may wonder about the practical interest of such theoretical developments. Moreover, one may also wonder about the physics relevance of the most probable action, I^*, we use to define ΔI. We will now answer these questions by showing that, indeed, I^* is useful to compute the imaginary part, χ_i, of the electron susceptibility for a plasma wave, and that χ_i will actually provide a very fine diagnostic for our prediction of ΔI. Moreover, we will show that, by using our perturbative results for χ_i, which are actually published in Ref. [10] and are much simpler than those giving the orbit in phase space, we are able to calculate ΔI for a larger range in I_0 than in Sec. II.

A. The electron susceptibility

The sinusoidal potential used in Hamiltonian H, Eq. (2), may be viewed as the potential of a sinusoidal electric field,

$$E = -i\frac{\Phi}{2}e^{ix} + \text{c.c.} \tag{8}$$

$$\equiv E_0 e^{ix} + \text{c.c.,} \tag{9}$$

where c.c. stands for the complex conjugate. This field induces, for example in a plasma, the charge density,

$$\rho = \rho_0 e^{ix} + \text{c.c.,} \tag{10}$$

and we introduce

$$\chi \equiv \frac{i\rho_0}{\varepsilon_0 E_0}, \tag{11}$$

so that, since E_0 only depends on time, Gauss law just reads

$$1 + \chi = 0. \tag{12}$$

Note that the electron susceptibility is usually defined in Fourier space, while we define here χ in the direct space, because the use of the Fourier representation is of little help to address the nonlinear regime of wave-particle interaction we focus on in this paper. The imaginary part of Eq. (12) simply yields $\chi_i = 0$, and, as shown in previous papers (see Ref. [15] and references therein), the resolution of this equation, with χ_i derived for an exponentially growing wave, could provide values of such quantities as Raman reflectivity in a plasma, or yield a very accurate description of the nonlinear propagation of an electrostatic wave. However, previous results for χ_i were only obtained in a nearly adiabatic situation, with a smooth distribution in the initial particles' velocity, so that phase mixing was effective enough to render negligible the contribution to χ_i from trapped particles (see Refs. [10,25]). We now want to calculate this contribution very precisely, which lets us choose an initial condition with the same initial velocity for all particles, so that phase mixing cannot occur.

Now, from Eq. (10), since ρ_0 only depends on time,

$$\rho_0 = \frac{1}{2\pi}\int_{-\pi}^{\pi}\rho e^{-ix}dx \tag{13}$$

$$= \frac{1}{2\pi}\int_{-\pi}^{\pi}\int_{-\infty}^{+\infty}F(x,v,t)e^{-ix}dx\,dv \tag{14}$$

$$\equiv \langle e^{-ix}\rangle, \tag{15}$$

where $F(x,v,t)$ is the particles' distribution function, and where $\langle\cdot\rangle$ stands for the statistical averaging over all the particles. Since, from Eq. (8), E_0 is purely imaginary, we conclude that χ_i is proportional to $\langle\sin(x)\rangle$, the quantity we focus on in the remainder of this paper. Note that, for a discrete set of particles, as considered in numerical simulations,

$$\langle\sin(x)\rangle = \frac{1}{N}\sum_{i=1}^{N}\sin(x_i), \tag{16}$$

where N is the total number of particles and x_i is the position of the ith particle.

B. Use of the global change in action to compute χ_i

1. Theoretical estimate of χ_i and comparisons with numerical results

In this subsection we show that, when I_0 is small enough, it is possible to compute χ_i [or $\langle\sin(x)\rangle$] by connecting perturbative estimates with adiabatic ones.

The perturbative estimate of $\langle\sin(x)\rangle$ is calculated at order 11 [23], and its value may be found in Ref. [10]. This estimate is used up to $\Phi = \Phi_M$, when $\langle\sin(x)\rangle$ reaches its first maximum, which we denote by S_M.

When $\Phi > \Phi_M$, we make use of the adiabatic approximation and, therefore, we shift to action-angle variables, (θ,I), and introduce $\tilde{f}(\theta,I,t) = F(x,v,t)$, the action-angle distribution function. Then,

$$\langle\sin(x)\rangle = \frac{1}{2\pi}\int_0^{2\pi}\int_0^{+\infty}\sin[x(\theta,I)]\tilde{f}(\theta,I,t)d\theta\,dI \tag{17}$$

since the change of variables $(x,v) \to (\theta,I)$ is canonical, so that its Jacobian is unity. We now assume that, by the time Φ reaches the value Φ_M, all the particles have been trapped in the potential. Then, using the formulas of θ and I for trapped particles (see Ref. [10]), we find

$$\sin(x) = 2\sin(x/2)\cos(x/2) \tag{18}$$

$$= 2\sqrt{m}\,\text{sn}\left[\frac{2K\theta}{\pi}\Big|m\right]\text{dn}\left[\frac{2K\theta}{\pi}\Big|m\right], \tag{19}$$

where $\text{sn}(u|m)$ and $\text{dn}(u|m)$ are Jacobian elliptic functions and $K \equiv K(m)$ is the complete elliptic integral of the first kind [26]. Using the Fourier representation of elliptic functions [26], we find

$$\sin(x) = 2\left\{\frac{2\pi}{K}\sum_{n=0}^{+\infty}\frac{q^{n+1/2}}{1-q^{2n+1}}\sin[(2n+1)\theta]\right\}$$

$$\times\left\{\frac{\pi}{2K}+\frac{2\pi}{K}\sum_{n=1}^{+\infty}\frac{q^n}{1+q^{2n}}\cos[2n\theta]\right\}, \tag{20}$$

where $q \equiv \exp[-\pi K(1-m)/K(m)]$. Note that $q < 1$ and that it rapidly decreases with m. Hence, if all the particles are deeply trapped when $\Phi > \Phi_M$, i.e., such that m is significantly less than unity, then $\sin(x)$ may be approximated by its first Fourier coefficient in θ, namely,

$$\sin(x) \approx \frac{2\pi^2}{K^2} \frac{\sqrt{q}}{1-q} \sin(\theta). \tag{21}$$

Now, in Sec. II we saw that, once all the particles have been trapped, the distribution in I exhibited one sharp peak and that, once $\langle \sin(x) \rangle$ has reached its first maximum, the most probable action was quite close to its asymptotic value, I_f. Consequently, we may approximate $\langle \sin(x) \rangle$ by assuming that, when $\Phi > \Phi_M$, all the particles have the same constant action, $I = I_f$. This allows us to relate the angle θ of each particle to the value, θ_M, reached at $t = t_M$ when $\Phi = \Phi_M$, by the same formula,

$$\theta(t) = \theta_M + \int_{t_M}^{t} \omega_0(I_f) dt', \tag{22}$$

with

$$\omega_0(I_f) = \frac{\pi \sqrt{\Phi}}{2K[m(I_f)]}, \tag{23}$$

and $m(I_f)$ is such that

$$\frac{4\sqrt{\Phi}}{\pi} \{E[m(I_f)] + [m(I_f) - 1]K[m(I_f)]\} = I_f, \tag{24}$$

where $E(m)$ is the elliptic integral of the second kind [26]. Equation (23) is just the well-known result for the frequency of a pendulum, while Eq. (24) expresses the fact that the particle's action is I_f [10].

To conclude the derivation of $\langle \sin(x) \rangle$, we use the Liouville theorem, $\tilde{f}(\theta, I, t) = \tilde{f}[\theta_M(\theta, I), I_M(\theta, I), t_M]$, we approximate the distribution in action by a δ function at $I = I_f$, and we expand $\tilde{f}(\theta_M, I_M)$ in Fourier series to find

$$\tilde{f}(\theta, I, t) = \tilde{f}[\theta_M(\theta, I), I_M(\theta, I), t_M]$$
$$= \sum_{n=0}^{+\infty} [f_{cn} \cos(n\theta_M) + f_{sn} \sin(n\theta_M)] \delta(I_M - I_f). \tag{25}$$

Plugging Eqs. (21) and (25) into the expression (17) for $\langle \sin(x) \rangle$, taking advantage of the fact that the Jacobian of the change of variables $(\theta, I) \to (\theta_M, I_M)$ is unity, and using the value of $\langle \sin(x) \rangle$ at $t = t_M$ when $\Phi = \Phi_M$ derived from perturbation theory, namely $\langle \sin(x) \rangle = S_M$ when $t = t_M$, we find

$$\langle \sin(x) \rangle = S_M \frac{K_M^2}{K^2} \sqrt{\frac{q}{q_M}} \frac{1-q_M}{1-q} \cos\left[\int_{t_M}^{t} \omega_0(I_f) dt'\right], \tag{26}$$

where K_M and q_M are the values of K and q when $\Phi = \Phi_M$. Note that, in Eq. (26), we did not account for the term proportional to $\sin[\int_{t_M}^{t} \omega_0(I_f) dt']$. This term should actually be negligible because the value reached by $\langle \sin(x) \rangle$ at $t = t_M$ is a local maximum, and $\int_{t_M}^{t} \omega_0(I_f) dt'$ varies much more rapidly with time than q. Therefore, the maxima of $\langle \sin(x) \rangle$ are identified with those of $\cos[\int_{t_M}^{t} \omega_0(I_f) dt']$.
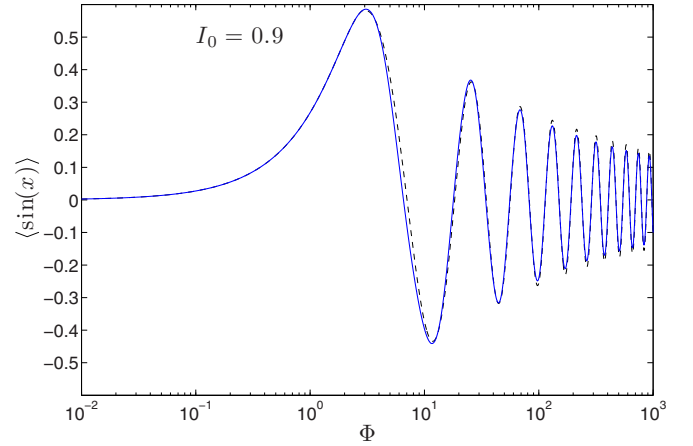

FIG. 8. (Color online) $\langle \sin(x) \rangle$ when $I_0 = 0.9$ as calculated numerically (blue solid line) and theoretically (black dashed line) by connecting the perturbative estimate with the values of $\langle \sin(x) \rangle$ given by Eq. (27).

We now make the change of variables $t \to \Phi$ in the integral of Eq. (26) to find, when Φ grows exponentially in time,

$$\langle \sin(x) \rangle \approx S_M \frac{K_M^2}{K^2} \sqrt{\frac{q}{q_M}} \frac{1-q_M}{1-q} \cos\left[\int_{\Phi_M}^{\Phi} \frac{d\Phi'}{\sqrt{\Phi'} K[m(I_f)]}\right], \tag{27}$$

where $m(I_f)$ is related to Φ by Eq. (24).

As shown in Fig. 8, the values of $\langle \sin(x) \rangle$ for $I_0 = 0.9$ obtained by using the perturbative estimate of Ref. [10] for $\Phi \leqslant \Phi_M \approx 3.08$, and Eq. (27) for $\Phi \geqslant \Phi_M$, agree very well with the numerical ones. To derive the value of I_f, we followed the method described in Sec. II, i.e., using a perturbation analysis, we estimated the most probable action when $\Phi = \Phi_M$. When doing so, we found $I_f \approx 0.495$, so that the global change in action, ΔI, is about 40% of I_0.

2. Use of χ_i as a diagnostic for ΔI

As shown in Fig. 8, $\langle \sin(x) \rangle$ oscillates very quickly with Φ so that a small error in the estimate of the frequency, ω_0, of these oscillations would entail a shift in the positions of the maxima of $\langle \sin(x) \rangle$ that would be rapidly visible. Therefore, one way to guess I_f numerically may consist in trying to match the locations of the maxima of $\langle \sin(x) \rangle$, obtained from numerical simulations, with those derived from Eq. (27). More precisely, we denote by Φ_n^{num} and Φ_n^{th}, respectively, the numerical and theoretical estimates of the amplitude at which $\langle \sin(x) \rangle$ reaches its nth maximum, and we introduce $\Delta_n \equiv \Phi_{n+1}^{num} - \Phi_n^{num}$ and $\delta_n = \Phi_n^{th} - \Phi_n^{num}$. Then, I_f is found numerically as the value that, when used in Eq. (27), makes the ratio δ_n/Δ_n as small as possible over a large number of oscillations. Numerically, it is very demanding to calculate $\langle \sin(x) \rangle$ up to very large amplitudes, and, to do so, we had to use a very small time step, $dt = 10^{-9}$. Figure 9 plots δ_n/Δ_n when $I_0 = 100$ and $I_f = 99.56$ (blue line) or $I_f = 100$ (green line). It shows that, when using $I_f = 99.56$ in Eq. (27) (with Φ_M and S_M obtained numerically), the positions of the maxima of $\langle \sin(x) \rangle$ remain very close to the numerical ones. Indeed, even after the 25 395 oscillations we calculated, they differ by
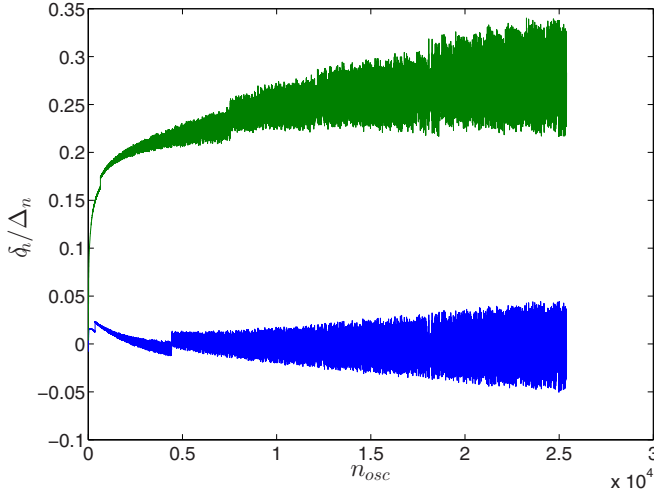
FIG. 9. (Color online) δ_n/Δ_n as a function of the number of oscillations, n_{osc}, when $I_0 = 100$, and by using in Eq. (27) $I_f = 99.56$ (blue lower line) or $I_f = 100$ (green upper line).

less than the uncertainty due to the discreteness of $\langle \sin(x) \rangle$, and the averaged value δ_n/Δ_n is found to be close to -8×10^{-4}. The good agreement between the values of Φ_n^{num} and Φ_n^{th} with $I_f = 99.56$ may also be appreciated in Fig. 10 [where we multiplied the amplitudes of $\langle \sin(x) \rangle$ given by Eq. (27) by a factor close to 0.8, because they were slightly overestimated by this equation for the large amplitudes considered in Fig. 10, as discussed in the end of Appendix]. Moreover, as shown in Figs. 9 and 10, neglecting the change in action and using $I_f = I_0 = 100$ instead of $I_f = 99.56$ does entail a shift in the locations of the maxima of $\langle \sin(x) \rangle$ that is clearly visible. Hence, in addition to being an important physics quantity, χ_i may be used as a very fine diagnostic that reveals a relative error in the particles' global action as small as 0.5%. Moreover, the results of Figs. 8–10 clearly show that the very concept of a global action for a set of particles is relevant to theoretically compute macroscopic quantities such as χ_i, and, in particular,
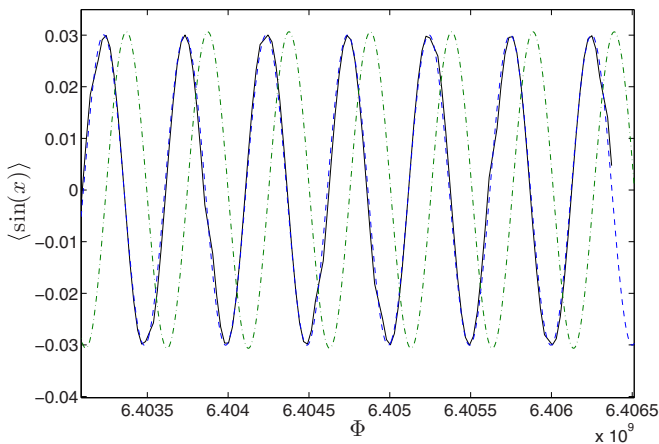

FIG. 10. (Color online) Comparisons between the values of $\langle \sin(x) \rangle$ when $I_0 = 100$ calculated numerically (black solid line) and by making use of Eq. (27) with $I_f = 99.56$ (blue dashed line) and $I_f = 100$ (green dash-dotted line) after 23 595 oscillations.

the contribution to χ_i from trapped particles. Actually, for the parameters of Fig. 9, making use of Eq. (27) reduces the computation time of $\langle \sin(x) \rangle$ by more than four orders of magnitude compared to a direct numerical resolution of the equations of motion.

C. Use of χ_i to compute the global change in action

In the preceding subsection, we saw that we could compute χ_i very efficiently by making use of the concept of global action, provided that ΔI was known. In Sec. II, ΔI was obtained theoretically, for small enough values of I_0, from the particles' distribution function derived by making use of a perturbation analysis. Now, it is much more difficult to derive the distribution function than to estimate one of its Fourier coefficient, so that the perturbative values of $\langle \sin(x) \rangle$, and in particular the estimates of Φ_M and S_M, are expected to be accurate for a larger range in I_0 than the distribution function itself. Moreover, from the perturbative estimate of $\langle \sin(x) \rangle$ it is possible calculate ΔI, as we will now show.

Plugging Eqs. (21), (22), and (25) into Eq. (17) yields

$$\langle \sin(x) \rangle = \pi^2 f_{s1} \frac{\sqrt{q}}{K^2(1-q)} \cos\left[\int_{t_M}^{t} \omega_0(I_f) dt' \right], \quad (28)$$

showing that the maxima of $\langle \sin(x) \rangle$ are proportional to $\sqrt{q}/K^2(1-q)$. Moreover, as discussed in Appendix, the coefficient f_{s1} depends very little on I_0, and it may therefore be considered as a constant. This is illustrated in Fig. 11 showing that the local maxima of $\langle \sin(x) \rangle$, when plotted as a function of m, lie on a curve that depends very little on I_0.

Therefore, each maximum S_{max} of $\langle \sin(x) \rangle$, occurring at $\Phi = \Phi_{\text{max}}$, is such that

$$S_{\text{max}} = S_0 \frac{\sqrt{q_{\text{max}}}}{K_{\text{max}}^2(1-q_{\text{max}})}, \quad (29)$$

where S_0 is a constant, and where $q_{\text{max}} \equiv q(m_{\text{max}})$ and $K_{\text{max}} \equiv K(m_{\text{max}})$, with m_{max} such that

$$\frac{4}{\pi}\sqrt{\Phi_{\text{max}}} [E(m_{\text{max}}) + (m_{\text{max}} - 1)K(m_{\text{max}})] = I_f. \quad (30)$$

Now, the first maximum, S_M, of $\langle \sin(x) \rangle$, and the amplitude, $\Phi = \Phi_M$, when it occurs, can be estimated by making use of our perturbation analysis in the wave amplitude [27]. Therefore, if the constant S_0 is known, one just has to solve Eq. (29) for m_{max} with $S_{\text{max}} = S_M$, and to plug the value thus found in Eq. (30) with $\Phi_{\text{max}} = \Phi_M$ in order to calculate I_f. To derive the constant S_0, we need to know the change in action, $\Delta I = I_f - I_0$, at least for one I_0, which we do by making use of the method described in Sec. II, and which yields $S_0 \approx 11.6$ [the accuracy of this estimate, further discussed in Appendix, may be appreciated in Fig. 11(a)]. With this value of S_0, we calculate the function $\Delta I(I_0)$ represented by the dashed curve in Fig. 6(a), and which appears to be accurate whenever $I_0 \lesssim 1.6$. To be more specific, when $I_0 = 1.6$ we find $\Delta I \approx -0.444$, which is to be compared with the numerical result $\Delta I \approx -0.437$ given at the end of Sec. II, and with the neoadiabatic estimate, $\Delta I = -(2/\pi)\ln(2) \approx -0.441$. We therefore conclude that, by making use of a perturbation analysis, it is possible to provide accurate estimates for the global change in action up to values of I_0 large enough
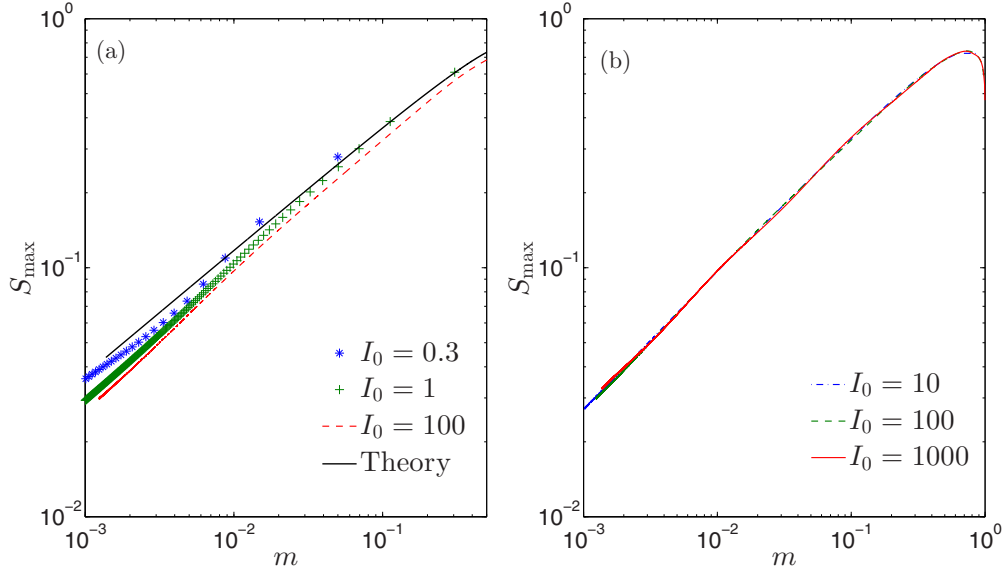
FIG. 11. (Color online) Local maxima, $S_{\max}$, of $\langle \sin(x) \rangle$ as a function of m for various values of I_0. The black solid curve in panel (a) plots the values given by Eq. (29) with $S_0 = 11.6$.

for the neoadiabatic estimate to be also very accurate. This shows that, indeed, the action change due to trapping can be calculated theoretically, regardless of the rate of variation of the dynamics, by connecting the perturbative results with the neoadiabatic ones.

IV. CONCLUSION

In this paper, we introduced the concept of a "global action" for a set of particles with the same initial action, I_0. This was done by showing that, when all the particles are trapped, the distribution in action, $f(I)$, has one very sharp peak, at the smallest action. In addition to numerical evidence, this result was proved theoretically by making use of a perturbation analysis in the potential amplitude, which is valid when $I_0 \lesssim 1$, and by making use of the neoadiabatic theory, which is already quite accurate when $I_0 \gtrsim 1$. Moreover, we showed that the global action we defined was relevant, and actually very useful, to efficiently compute macroscopic quantities, such as the imaginary part, χ_i, of the electron susceptibility for a plasma wave. In particular, we could compute very accurately χ_i whether the particles were trapped or untrapped, even when the particles' motion was far from adiabatic before trapping, a result that was not available in previous publications [10,25,28]. As for the change in action, $\Delta I = (I_f - I_0)$, we could derive it regardless of the rate of variation of the dynamics and, in particular, for a non-slowly-varying dynamics, when ΔI was not small compared to I_0. Our derivation of ΔI rests mainly on a perturbative expansion, in the potential amplitude, of the particles' motion. More precisely, it is derived by plugging the perturbative estimate of the first maximum, $S_{\max} \equiv S_M$, of $\langle \sin(x) \rangle$ (which is proportional to χ_i), and of the corresponding value of the potential amplitude, $\Phi_{\max} \equiv \Phi_M$, into Eqs. (29) and (30) with $S_0 \approx 11.6$. These equations provide an accurate estimate of ΔI up to the point when it becomes essentially independent of I_0, and nearly matches the constant value $\Delta I \approx -(2/\pi) \ln(2)$

provided by the neoadiabatic theory. The latter value was, moreover, found to be in excellent agreement with numerical results when $I_0 \gg 1$.

In conclusion, this paper shows the following two main results: (i) The notion of a global action and its relevance to theoretically compute macroscopic quantities such as χ_i; (ii) the theoretical derivation of the global change in action due to trapping, whether the dynamics is slowly varying or not. Moreover, as will be shown in a forthcoming paper, the results derived here, particularly those with regard to the theoretical estimate of χ_i, constitute an essential step to describe the nonlinear regime of the beam-plasma instability and to theoretically compute the nonlinear Landau damping rate of a plasma wave, which are long-standing issues in plasma physics.

ACKNOWLEDGMENTS

APPENDIX: SHIFT IN ANGLE COMPARED TO A PURELY ADIABATIC MOTION

In this Appendix we show that, once the action is very close to its asymptotic value, $I \approx I_0 - \Delta I$, the variation in angle compared to purely adiabatic motion is essentially independent of I_0 in the limit $I_0 \to \infty$. This proves that, once the action has converged toward a nearly constant value, the distribution in angle, which would have been uniform for a purely adiabatic motion, changes in a fashion that is essentially independent of I_0. Consequently, the Fourier component of this distribution, which we denoted by f_{s1} in Sec. III, is essentially independent of I_0, so that the factor S_0 in Eq. (29) for $\langle \sin(x) \rangle$ is indeed a constant, as illustrated in Fig. 11 of Sec. III.

To show the aforementioned results, we calculate the variation in angle up to a time, t_t, when the shift in action has reached its asymptotic value, ΔI, and the particles are deeply trapped [since Eq. (29) on Sec. III is only valid in this limit]. In action-angle variables, the dynamics is ruled by the Hamiltonian

$$\mathcal{H}(\theta, I) = H + \frac{\partial F}{\partial t}, \tag{A1}$$

where H is defined by Eq. (2), and where F is the generative function of the canonical change of variables, $(x, v) \rightarrow (\theta, I)$. Calculating the change in angle by making use of the adiabatic approximation amounts to neglecting the term $\partial F / \partial t$ in $\mathcal{H}$, so that I remains a constant. Then, for an untrapped particle,

$$\frac{d\theta}{dt} = \frac{\pi \sqrt{\Phi}}{2 \sqrt{m_1} K(m_1)}, \tag{A2}$$

where m_1 is related to the action and the amplitude by

$$\frac{4 \sqrt{\Phi}}{\pi \sqrt{m_1}} E(m_1) = I, \tag{A3}$$

while, for a trapped particle,

$$\frac{d\theta}{dt} = \frac{\pi \sqrt{\Phi}}{2 K(m)}, \tag{A4}$$

with

$$\frac{4 \sqrt{\Phi}}{\pi} [E(m) + (m - 1) K(m)] = I. \tag{A5}$$

Using $d\Phi/dt = \Phi$, one easily finds that the adiabatic change in angle, which we denote by $\Delta\theta_a$, is

$$\Delta\theta_a = \frac{\pi^2}{8} \left\{ \int_{m_{\min}}^1 \frac{I}{m_1 E^2} dm_1 + \int_{m_t}^1 \frac{I}{[E + (m-1)K]^2} dm \right\}, \tag{A6}$$

where the first term accounts for the variation of the angle while the particle is untrapped, and the second term is the angle variation when the particle is trapped. In Eq. (A6), $m_{\min}$ is the value of m_1 defined by Eq. (A3) at $t = 0$ when $\Phi = \Phi_0$ and $I = I_0$. As for m_t, it is the value of m defined by Eq. (A5) at time t_t when, for the true nonadiabatic dynamics, the action is very close to its asymptotic value, i.e., $I \approx I_0 - \Delta I$.

Now, using the Hamiltonian $\mathcal{H}$ defined by Eq. (A1), one finds

$$\frac{d\theta}{dt} = \frac{dH}{dI} + \frac{\partial}{\partial I}\left(\frac{\partial F}{\partial t}\right), \tag{A7}$$

so that the shift in angle compared to a purely adiabatic motion, which we denote by $\delta\theta$, may be seen as the sum of two contributions. The first one, $\delta\theta_1$, is obtained by accounting for the change in action when calculating $\int (dH/dI) dt$. Hence, $\delta\theta_1$ is just the shift in $\Delta\theta_a$ entailed by the change in action, which we denote by $\delta\theta_1 \equiv \delta(\Delta\theta_a)$. As for the second contribution to $\delta\theta$, which we denote by $\delta\theta_2$, it is defined by

$$\frac{d\delta\theta_2}{dt} = \frac{\partial^2 F}{\partial I \partial t}. \tag{A8}$$

Let us first estimate $\delta\theta_1 \equiv \delta(\Delta\theta_a)$, which, from Eq. (A6), is given by

$$\delta\theta_1 = \frac{\pi^2}{8} \left\{ \int_{m_{\min}}^1 \delta\left[\frac{I}{mE^2}\right] dm + \int_{m_t}^1 \delta\left[\frac{I}{[E + (m-1)K]^2}\right] dm \right. \\ \left. - \frac{I \delta m_t}{[E + (m_t - 1)K]^2} \right\}. \tag{A9}$$

Let us now denote by δI_m the instantaneous change in action when the wave amplitude assumes the value Φ, i.e., $\delta I_m \equiv I[m(\Phi)] - I_0$. From Eq. (A3), it is easily found that when the particle is untapped, the change δI_m entails a change in m_1 by

$$\delta m_1 = -\frac{2 m_1 E}{K} \frac{\delta I_m}{I}, \tag{A10}$$

while when the particle is trapped, one finds from Eq. (A5)

$$\delta m = \frac{2[E + (m-1)K]}{K} \frac{\delta I_m}{I}. \tag{A11}$$

Plugging the results from Eqs. (A10) and (A11) into Eq. (A9), one easily finds

$$\frac{8 \delta\theta_1}{\pi^2} = \int_{m_{\min}}^1 \frac{\delta I_m}{m_1 E^2} \left[\frac{4E}{K} - 1\right] dm_1 \\ - \int_{m_t}^1 \frac{\delta I_m}{[E + (m-1)K]^2} dm - \frac{2 \delta I_{m_t}}{K[E + (m_t - 1)K]}. \tag{A12}$$

When the particle is untrapped, δI_m is negligible except close to the separatrix, where it scales as $\ln(I_0)$ when $(1 - m) \sim 1/I_0$. Similarly, when the particle is trapped, then within a narrow region close to the separatrix where $(1 - m) \sim 1/I_0$, δI_m scales as $\ln(I_0)$. However, away from this narrow region, δI_m for a trapped particle is very close to its asymptotic value, ΔI. Hence, one finds

$$\delta\theta_1 = -\frac{\pi^2 \Delta I}{8} F(m_t) + O\left[\frac{\ln(I_0)}{I_0}\right], \tag{A13}$$

where

$$F(m_t) = \int_{m_t}^1 \frac{dm}{[E + (m-1)K]^2} + \frac{2}{K[E + (m_t - 1)K]}. \tag{A14}$$

For large I_0's, since ΔI becomes essentially independent of I_0, it is clear from Eq. (A13) that so does $\delta\theta_1$.

Let us now calculate $\delta\theta_2$, defined by Eq. (A8). Using

$$F = \pm \int_0^x \sqrt{2[H + \Phi \cos(u)]} du \tag{A15}$$

together with $d\Phi/dt = \Phi$, one easily finds

$$\frac{\partial F}{\partial t} = \theta \frac{\partial H/\partial t - H}{\partial H/\partial I} + \frac{F}{2}. \tag{A16}$$

Note that, in Eq. (A8), F is considered as a function of θ and I so that, in Eq. (A15), $x \equiv x(\theta, I)$, such that, for an untrapped electron,

$$\sin(x/2) = \text{sn}(2K\theta/\pi), \tag{A17}$$

while for a trapped electron,

$$\sin(x/2) = \sqrt{m}\,\text{sn}(2K\theta/\pi). \quad (A18)$$

Then, using the fact that, for an untrapped electron, H and I read $H \equiv h_u(m_1)\Phi$, $I \equiv \mathcal{I}_u(m_1)\sqrt{\Phi}$ [while, for a trapped electron, $H \equiv h_t(m)\Phi$, $I \equiv \mathcal{I}_t(m)\sqrt{\Phi}$], one easily finds

$$\frac{\partial^2 F}{\partial I \partial t} = \frac{1}{2}\frac{\partial F}{\partial x}\frac{\partial x}{\partial I}. \quad (A19)$$

Then, Eqs. (A8), (A15), (A19), and (A17) yield, for an untrapped electron,

$$\frac{d\delta\theta_2}{dt} = \frac{\pi}{4(m-1)K}\text{dn}(\upsilon)[\text{dn}(\upsilon)Z(\upsilon) - m\,\text{sc}(\upsilon)\text{cn}^2(\upsilon)], \quad (A20)$$

where we have denoted $\upsilon \equiv 2K\theta/\pi$, and where the functions appearing in Eq. (A20) are the well-known Jacobian elliptic functions [26]. Similarly, for a trapped electron, it comes from Eqs. (A8), (A15), (A19), and (A18) that

$$\frac{d\delta\theta_2}{dt} = \frac{\pi}{4K}\text{cn}(\upsilon)\left[(m-1)\text{sd}(\upsilon) + \frac{\text{sd}(\upsilon)\text{cn}^2(\upsilon)}{m-1}\right.$$
$$\left. + \frac{\text{cn}(\upsilon)Z(\upsilon)}{m-1}\right]. \quad (A21)$$

Hence, $d\delta\theta_2/dt$ is an oscillating function with period 2π in θ. In the limit when $I_0 \to \infty$, θ varies much more rapidly with

time than m so that $\delta\theta_2$ nearly averages out to zero any time θ is a multiple of 2π. Hence, since $d\theta/dt$ is proportional to I_0, $\delta\theta_2$ is expected to decrease as $1/I_0$ and become negligible as $I_0 \to \infty$.

In conclusion, for large enough values of I_0, and once the action is very close to its asymptotic value, $I \approx I_0 - \Delta I$, the shift in angle compared to a purely adiabatic motion, $\delta\theta = \delta\theta_1 + \delta\theta_2 \approx \delta\theta_1$, is a function of m that is independent of I_0. Since the distribution in θ would have been uniform if the motion were adiabatic, its Fourier coefficient f_{s1}, defined by Eq. (25), is also a function of m that becomes independent of I_0 in the limit $I_0 \to \infty$. This is in total agreement with the results of Fig. 11 in Sec. III.

Note that f_{s1} is necessarily less than unity, while we used $\pi^2 f_{s1} \equiv S_0 \approx 11.6$ in Eq. (29). This value was used in order to derive precisely the amplitude of the first maximum of $\langle\sin(x)\rangle$, which occurs for an amplitude that is not large enough for the approximate expression of $\sin(x)$ given by Eq. (21) of Sec. III to be extremely accurate (although it is already a good approximation). For subsequent maxima, which occur for large amplitudes and, therefore, small values for m, the expression for $\langle\sin(x)\rangle$ given by Eq. (28) becomes very accurate, and, in this expression, f_{s1} is necessarily a constant (independent of m) less than unity. This explains why, in Fig. 10 of Sec. III, we had to multiply the amplitude of $\langle\sin(x)\rangle$, as given by Eq. (27), by a constant close to 0.8 in order to match the numerical results (and one may actually notice that $\pi^2/11.6 \approx 0.85$).

[1] A. Lenard, Ann. Phys. (NY) **6**, 261 (1959).

[2] A. Neishtadt, Sov. Phys. Dokl. **20**, 189 (1975).

[3] J. R. Cary, D. F. Escande, and J. L. Tennyson, Phys. Rev. A **34**, 4256 (1986).

[4] X. Leoncini, A. Neishtadt, and A. Vasiliev, Phys. Rev. E **79**, 026213 (2009).

[5] A. Bazzani, C. Frye, M. Giovannozzi, and C. Hernalsteens, Phys. Rev. E **89**, 042915 (2014).

[6] A. Neishtadt, Celestial Mech. Dyn. Astron. **65**, 1 (1997).

[7] R. Cappi and M. Giovannozzi, Phys. Rev. Lett. **88**, 104801 (2002).

[8] A. P. Itin and S. Watanabe, Phys. Rev. E **76**, 026218 (2007).

[9] I. Y. Dodin and N. J. Fisch, Phys. Rev. Lett. **107**, 035005 (2011).

[10] D. Bénisti and L. Gremillet, Phys. Plasmas **14**, 042304 (2007).

[11] D. Bénisti, D. J. Strozzi, and L. Gremillet, Phys. Plasmas **15**, 030701 (2008).

[12] D. Bénisti, D. J. Strozzi, L. Gremillet, and O. Morice, Phys. Rev. Lett. **103**, 155002 (2009).

[13] D. Bénisti, O. Morice, L. Gremillet, and E. Siminos, Phys. Plasmas **17**, 082301 (2010).

[14] D. Bénisti, O. Morice, L. Gremillet, E. Siminos, and D. J. Strtozzi, Phys. Plasmas **17**, 102311 (2010).

[15] D. Bénisti, O. Morice, and L. Gremillet, Plasmas **19**, 063110 (2012).

[16] D. Bénisti, O. Morice, L. Gremillet, E. Siminos, and D. J. Strozzi, Phys. Rev. Lett. **105**, 015001 (2010).

[17] D. Bénisti, O. Morice, L. Gremillet, A. Friou, and E. Lefebvre, Phys. Plasmas **19**, 056301 (2012).

[18] D. Bénisti and L. Gremillet, Discontin. Nonlin. Complex. **3**, 435 (2014).

[19] M. D. Rosen et al., High Energy Density Phys. **7**, 180 (2011).

[20] D. Bénisti, CEA report, R-6269 (2011).

[21] One may think of introducing the new time $t' \equiv e^{t/2}$ in order to study the dynamics of H. When doing so, one finds the equation of a damped pendulum, $\frac{d^2 x}{dt'^2} = -4\Phi_0 \sin(x) - \frac{dx/dt'}{t'}$, which we investigated but did not find very useful.

[22] L. Verlet, Phys. Rev. **159**, 98 (1967).

[23] There was, a priori, no reason to stop at order 12, except the memory limitations we had to face when running our routine for symbolic computation. However, going to order 12 was enough for the purpose of this paper, and, therefore, we did not try to go beyond this order. With regard to the computation of $\langle\sin(x)\rangle$, only odd orders give a nonzero contribution so that its value at order 11 is the same as that obtained at order 12.

[24] Y. Elskens and D. F. Escande, Nonlinearity **4**, 615 (1991).

[25] D. Bénisti, N. A. Yampolsky, and N. J. Fisch, Phys. Plasmas **19**, 013110 (2012).

[26] Handbook of Mathematical Functions, 10th ed., edited by M. Abramowitz and I. A. Stegun (Dover, New York, 1972), pp. 569–626.

[27] When plotting the perturbative estimate of $\langle\sin(x)\rangle$ as a function of Φ, we actually only find a local maximum when $I_0 \lesssim 1.2$, which is a defect of the perturbative expansion. When $I_0 \gtrsim 1.2$, the first maximum of $\langle\sin(x)\rangle$, and the amplitude when it is reached, are estimated by the point at which the slope of $\langle\sin(x)\rangle(\Phi)$, as calculated perturbatively, is minimum. This estimate remains accurate as long as $I_0 \lesssim 1.6$, and, for these values of I_0, it does provide a good estimate of the jump in action, as shown in Sec. III.

[28] I. Y. Dodin and N. J. Fisch, Phys. Plasmas **19**, 012102 (2012).